A novel diagnostic methodology for fuel cell stack health: Performance, consistency and uniformity

Zunyan Hu[a], Liangfei Xu[a,**], Jianqiu Li[a,*], Quanquan Gan[a,b], Xin Xu[b], Ziyou Song[a,c], Yangbin Shao[a], Minggao Ouyang[a]

[a] *State Key Lab of Automotive Safety and Energy, Tsinghua University, Beijing 100084, China*
[b] *Shanghai Shen-li High Tech Co., Ltd., Yuandong Rd., Industry Comprehensive Development Zone, Shanghai, China*
[c] *Department of Electric Engineering and Computer Science, University of Michigan, Ann Arbor, MI 48109, USA*

A B S T R A C T

Internal heterogeneity is a significant challenge to the service life of large-format commercial fuel cell stacks. Methods for diagnosing fuel cell stack health, however, are still lacking. This paper proposes a novel diagnostic methodology for analyzing the performance, the consistency between cells and the uniformity within individual cells of fuel cell stacks. Specifically, this three-step methodology can comprehensively analyze the internal heterogeneity of large-format multi-cell stacks. First, a polarization curve test is conducted to provide a quick qualitative performance analysis. Then, the quantitative parameters consistency decline is analyzed by galvanostatic charging and electrochemical impedance spectroscopy methods. Finally, a novel multi-point voltage monitoring method is applied to rule out possible misdiagnoses and to qualitatively analyze cell uniformity. This degradation diagnostic methodology is applied to analyze degradation in several fuel cell stacks, revealing high potential in practice.

1. Introduction

Increasing awareness of environmental pollution and the growing energy crisis have spurred interest in developing new energy technologies for automobiles [1]. The fuel cell hybrid vehicle [2], with its long range [3] and low environmental impact [4], has been recognized by many governments and research institutions. However, the cost and lifetime of proton exchange membrane fuel cell stacks remain the primary bottlenecks for the commercialization [5]. In particular, the lifetime was a key challenge in early demonstrations [6]. How to clarify and relieve the degradation process in commercial fuel cell stacks is important for high-power fuel cell stack development [7].

1.1. Fuel cell degradation mechanism

Previous research has greatly contributed to understanding the fundamental degradation mechanisms of fuel cells [8] and analyses of system durability [9]. The reasons for the degradation of many components are increasingly clear, including the proton exchange membrane [10], catalyst layer [11], gas diffusion layer (GDL) [12], and bipolar plates [13]. However, only understanding the material degradation mechanisms is not enough for analyzing the degradation of entire fuel cell stacks [14]. Similar to lithium ion battery packs, the lifetime of commercial fuel cell stacks is shorter than that of small single cells, which is why the internal heterogeneity of a fuel cell stack can accelerate the decline in performance decline [15].

The degradation mechanism of high-power fuel cell stacks is more complex than that of experimental single cells [16]. The internal substance distribution between cells and along gas channels in one cell can be totally different [17]. Clarifying the degradation process of the consistency between cells and the uniformity within individual cells can help improve the lifetime of commercial fuel cell stacks.

Cell inconsistency is a key factor causing the performance decline of multi-cell stacks. Li et al. [18] analyzed the degradation process of a high-power fuel stack and found that the resistance of the cells in the middle region increases faster than that in the other regions. Jang et al. [19] also found that the performance of the center fuel cells is relatively lower than that of cells on the sides of the stack, which is determined by an inconsistent temperature distribution. Park et al. [20] studied different cooling methods to optimize the temperature consistency. They

Nomenclature		S_{ECSA}	electrochemical surface area
		l	bipolar plate length
h	bipolar plate height	δ	bipolar plate thickness
σ	resistant coefficient of graphite	i_0^{ref}	exchange current density
i_{ref}	reference current	T_{fc}	operating temperature
i_{lim}	limitation current	R	gas constant: 8.31 J/(mol·K)
α_c	cathodic transfer coefficient, 1	r	resistance
F	faraday constant, 96,485 C/mol	C_{dl}	double-layer capacitance
dQ_H	desorption proton quantity	i_{H_2}	hydrogen crossover current

found that the cell temperature at the center could increase from around 60 °C to 85 °C, which significantly affects the performance. Li et al. [21] analyzed temporary changes in the voltage consistency during dynamic loading. They proposed that the uneven distribution of liquid water in the diffusion layer caused a difference in the diffusion coefficients of each cell. Thus, cell inconsistency is a very common failure mode for multi-cell stacks. The performance decline of any cell in a high-power stack can limit the largest output current, and the lifetime of fuel cell stack is determined by the worst cell. Therefore, how to improve the cell consistency is important for multi-cell fuel cell stacks.

Cell uniformity is another significant challenge for long-lifetime commercial fuel cell stacks [22]. In order to enhance the power density, the effective area of commercial fuel cells is much larger than that of an experimental single cell [23]. Considering the mass transport and re-action consumption [24], the internal status in a single cell is non-uniform [25]. Hou et al. [26] studied the failure modes of commercial fuel cell stacks. Because of the start–stop cycle and fuel starvation, the degradation rate of GDL in the anode outlet region is faster than that in other regions. Xing et al. [27] analyzed the non-uniform temperature distributions inside the MEA (membrane electrode assembly) and channels at various stoichiometric flow ratios. Flooding is unavoidable in the cathode outlet, and an optimized channel structure and control strategy were proposed to improve the uniformity [28]. Yang et al. [29] proposed an in-plane transport effect on hydrogen depletion and carbon corrosion, which is induced by anode flooding. Local hydrogen star-vation may lead to in-plane current and substance flow. Hu et al. also analyzed the degradation mechanism under fuel starvation, and they found that only the catalyst layer in the anode outlet region was cor-roded [30]. Thus, according to previous research, the degradation of large-format fuel cell stacks due to non-uniformity in cells cannot be ignored. This non-uniformity is the main difference between the de-gradation mechanisms of the experimental single cell and those of fuel cell stacks.

In conclusion, the material degradation mechanisms alone cannot be used to comprehensively analyze the degradation of large-format commercial fuel cell stacks. From experimental work to commercial products, studies on cell consistency and uniformity leave this problem unresolved.

1.2. Fuel cell diagnostic methods

Suitable in situ diagnostic methods for analyzing cell consistency and uniformity are the basis for optimizing commercial fuel cell stack durability [31]. Note that diagnostic methods for commercial fuel cell stack are stricter than those used for experimental fuel cell stacks or single fuel cells.

Traditionally, the polarization curve test is the most convenient method for analyzing performance [32]. Voltage monitoring can pro-vide an individual voltage–current curve for each cell. Normally, the voltage loss in a polarization curve can be separated into three parts, i.e., the a) kinetic [33], b) ohmic [34], c) transport overpotentials [35]. Mench et al. [36] proposed a simple zero-dimensional cell model to use the polarization curve or ΔV curve to identify degradation mechanisms.

Zenyuk et al. [37] proposed a two-dimensional, multi-phase, transient model to study changes in the fuel cell stack performance. Further, Pant et al. [38] used this model to develop a simple, rapid diagnostic method. By sensing the oxygen concentration, this tool analyzes changes in the polarization curves of a cell over its lifetime to identify the main factor causing degradation. However, the accuracy of these methods depends on the accuracy of the model parameters [39], and it cannot provide any indication of changes in the cell uniformity.

Electrochemical impedance spectroscopy (EIS) is another popular diagnostic method for fuel cell stacks [40]. Yuan et al. [41] used EIS to analyze a five-cell stack under different temperatures, flow rates, and humidity levels. Next, they compared the EIS results of a fuel cell stack and individual cells [42] and validated its applicability to analyzing cell consistency. Darowicki et al. [43] comprehensively analyzed changes in the parameters of a fuel cell equivalent circuit using dynamic EIS to optimize the operating conditions. Martin et al. [44] applied EIS to estimate changes in the ohmic resistance and charge transfer resistance of the fuel cell under dry operating conditions. Unfortunately, the fit-ting results from EIS also depend on the equivalent circuit model [45]. Furthermore, the low-frequency test results of EIS are very sensitive to the operating conditions. Therefore, EIS is more suitable for qualitative analysis than quantitative analysis.

The galvanostatic charge method (GSC) is a very promising diag-nostic method for analyzing consistency in multi-cell stacks. Lee et al. [46] developed a galvanostatic analysis technique to estimate the electrochemical surface area (ECSA), crossover current, and double-layer capacitance, and they applied it to a single fuel cell stack and a five-cell PEMFC stack. However, they pointed out that the accuracy of this new method is unstable. Pei et al. [47] validated this method under different test conditions, and their results showed reasonable trends. Based on this method, Brightman et al. [48] evaluated the performance of an 18-cell PEMFC stack, and Torija et al. [49] analyzed the basic characteristics of a six-cell PEMFC stack. Further, Hu et al. [30] opti-mized the accuracy of this new technology using computations and a new test method. Their work was strictly validated using a four-cell stack. As a whole, GSC can effectively diagnose cell consistency, and the accuracy of this test is the only bottleneck.

Most of the classic methods to analyze the cell uniformity are used only in experimental research. Freunberger et al. [50] designed a spe-cialized two-cell stack with advanced localized diagnostics. Two cells operated in parallel, and unequal operation of the cells caused an in-plane current in the bipolar plate. Abbou et al. [51] proposed a seg-mented linear cell with reference electrodes to simultaneously monitor the local potentials and current densities during dead-ended anode operation. On the cathode side, 20 electrically insulated segments were used to collect the current distribution. Based on the cell uniformity analyses, some optimization strategies were devised to solve anode starvation [52]. Yang et al. [53] designed an experimental technique to simultaneously measure the species concentration and current density distributions. Some researchers even used advanced neutron imaging [54] and fluorescence microscopy techniques [55]. However, all of the abovementioned test technologies require specially designed bipolar plates or equipment, which are very expensive and affect the actual performance. Moreover, they are unpractical for commercial fuel cell

stacks. Recently, Hu et al. [56] proposed a multi-point voltage monitoring method to analyze the fuel cell consistency and uniformity in situ. Two sets of voltage monitors were placed along the channel, and the current and voltage redistribution process in a multi-cell stack could be observed in situ. This method cannot have a negative impact on fuel cell stacks and can be very convenient. It was used to explain how anode flooding affects the fuel cell performance [57]. Cell uniformity of commercial fuel cell stacks is still the largest challenge for in situ diagnosis. However, this multi-point monitoring method provides a possible approach to solving this problem.

In summary, previous studies have provided many useful diagnostic methods to analyze fuel cell degradation. However, most of these methods cannot directly analyze degradation in commercial fuel cell stacks. Thus, an in situ diagnostic methodology to analyze the cell consistency and uniformity of commercial fuel cell stacks remains lacking and immethodical. While a diagnostic methodology for commercial fuel cell stacks is urgently needed, it should be convenient and inexpensive.

This paper proposes a novel diagnostic methodology for large-format fuel cell stacks, focusing on the analysis of internal heterogeneity. This new methodology consists of three easy-to-follow steps. Section two introduces this methodology in detail. In addition, the diagnostic methods in the three steps are analyzed, and a degradation analysis framework is proposed. Section three presents the conclusion.

2. Degradation analysis system for multi-cell stacks

Commercial fuel cells are much larger than laboratory cells, and the consistency between cells and the uniformity of each cell are significant to degradation analysis. For a commercial fuel cell stack, individual components cannot be easily replaced, and the degree to which materials degrade is unknown. Thus, developing a suitable in situ analysis methodology for large-scale commercial fuel cell stacks is very important.

Fig. 1 shows the ideal frame diagram for analyzing commercial fuel cell stacks. In this three-step methodology, step one attempts to provide a brief diagnosis of the health status of the fuel cell stack. A quantitative analysis is not necessary at this stage, but it should be convenient and inexpensive for daily diagnosis. Next, step two should provide a detailed analysis of the consistency in the degradation rates of individual cells. The decline in the core indexes of each cell should also be analyzed. Finally, step three can clarify the cell uniformity degradation of the failed cell.

Based on considerable experimental experience, this paper proposes a detailed diagnostic methodology for analyzing the degradation of commercial fuel cell stacks. From step one to step three, some interesting and useful technologies are used to analyze degradation.

2.1. Step one: performance analysis

Step one requires a rapid, convenient test method for daily fuel cell stack diagnosis. Normally, voltage loss can be divided into the ohmic, activation, and concentration overpotentials. The key to this step is finding which part is the main factor and deciding whether it is necessary to conduct the rest of the steps. Recording a polarization curve is the most convenient in situ approach to monitoring daily performance degradation. According to the voltage variation under different output currents, this method can provide a qualitative analysis of the three parts of the overpotential.

$$
\begin{cases}
\Delta U_{act} = \frac{RT_{fc}}{\alpha_c F} \ln\left(\frac{i}{i_0^{ref} \times S_{ECSA2}} \right) \ - \ \frac{RT_{fc}}{\alpha_c F} \ln\left(\frac{i}{i_0^{ref} \times S_{ECSA1}} \right) \ = \frac{RT_{fc}}{\alpha_c F} \ln\left(\frac{S_{ECSA1}}{S_{ECSA2}} \right) \\[2ex]
\Delta U_{ohm} = i \times (r_2 - r_1) = i \times \Delta r \\[2ex]
\Delta U_{con} \approx \frac{RT_{fc}}{\alpha_c F} \ln\left(\frac{i_{ref}}{i_{\lim 2} - i} \right) \ - \ \frac{RT_{fc}}{\alpha_c F} \ln\left(\frac{i_{ref}}{i_{\lim 1} - i} \right) \ = \frac{RT_{fc}}{\alpha_c F} \ln\left(\frac{i_{\lim 1} - i}{i_{\lim 2} - i} \right) \\[2ex]
\qquad = \frac{RT_{fc}}{\alpha_c F} \ln\left(1 + \frac{i_{\lim 1} - i_{\lim 2}}{i_{\lim 2} - i} \right) \\[2ex]
\qquad\qquad\qquad = \frac{RT_{fc}}{\alpha_c F} \ln\left(1 + \frac{\Delta i_{\lim}}{i_{\lim 2} - i} \right)
\end{cases}
$$

$$(1)$$

Eq. (1) mathematically explains the degradation characteristics of the three kinds of overpotentials [18], where ΔU_{act}, ΔU_{ohm}, and ΔU_{con} are increasing overpotentials. All variables are defined in the nomenclature section. Actually, the degradation characteristics of the three types of overpotential are significantly different. For the activation overpotential, the performance decline is determined by the ECSA drop, S_{ECSA1}/S_{ECSA2}. Therefore, the voltage declines resulting from the activation overpotential under different currents are the same. For the ohmic overpotential, the voltage decline is linearly related to the output current. However, for the concentration overpotential, the voltage drop is more complicated, as its rate of increase becomes increasingly high with the increasing output current.

In order to clarify the three parts, Fig. 2a) shows the extra overpotential increasing under different output current. A 50% ECSA reduction, 0.03 $\Omega \cdot cm^2$ resistance increase, and 40% limitation current decrease are assumed for the fuel cell stack. The figure shows that the activation loss is constant, and the ohmic loss increases linearly. However, the increasing concentration loss is very complex. In the low-current region, the overpotential increases very slowly and almost linearly. Meanwhile, in the high-current region, the voltage decline exhibits nearly exponential growth. Therefore, there is a source of confusion in the polarization curve analysis method. Because the degradation mechanisms are coupled in fuel cell stacks, this curve may confuse the ohmic and activation overpotentials in the low-output-current region. It is hard to determine whether a fitting result is accurate with these specific models and parameters. In addition, a small voltage error in the activation overpotential can lead to a very large difference in the ECSA estimation. Therefore, more advanced technologies should be used to validate the results of analyzing the polarization curve.

Fig. 2b) presents an example of the polarization curve analysis. There are two polarization curves from a 10 kW fuel cell stack. The black and red lines are the polarization curves tested in 2015 and 2016, respectively. A voltage drop of approximately 70 mV voltage drop was observed in all working ranges, which represents a loss in the ECSA of nearly 70%, according to Eq. (1). This diagnosis is consistent with later performance tests, which revealed that the performance this fuel cell stack increasingly degraded in 2016, and the limitation current also dropped rapidly. Such analysis provided a prediction of the performance decline, and it is very effective and convenient for estimating the health of large-format multi-cell fuel cell stacks.

Actually, the polarization curve is similar to a grey box model. Accurately estimating each part depends on the model parameter definitions. Nevertheless, the polarization curve is the best way to make a quick qualitative judgment of multi-cell stacks. However, the polarization curve cannot provide a detailed diagnosis of the reason for the components' degradation. For example, both the ECSA drop and GDL
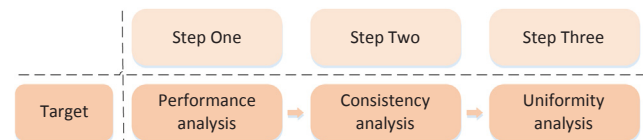

Fig. 1. Frame diagram of a conventional analysis process.

a) Comparison of the activation, ohmic, and

concentration overpotentials

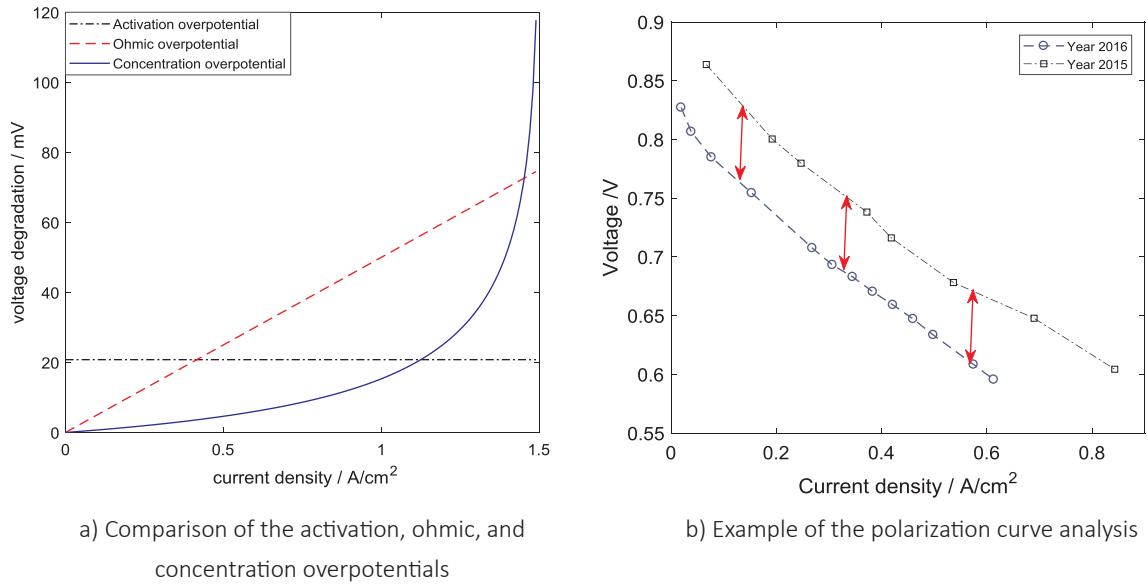b) Example of the polarization curve analysis

Fig. 2. Fuel cell overpotential analysis.

degradation can lead to increases in the concentration overpotential. Therefore, each cell must be quantitatively analyzed.

2.2. Step two: consistency analysis

The quantitative analysis of cell consistency is important but difficult for multi-cell stacks. In a multi-cell stack, the degradation degree of each cell is totally different. Some model-based methods can estimate changes in the internal parameters of each cell, but how to build these models is controversial in different papers. Thus, a more reliable analysis method to analyze consistency is the core of this step. To analyze the consistency, the resistance, ECSA, crossover current, and double-layer capacitance are chosen as key indexes, which can help to evaluate the degradation degree of each component.

The resistance measurement method is mature for multi-cell stacks. Whether using current interruption or EIS, obtaining the real-time resistance is easy. In this paper, the high-frequency impedance in EIS is used to measure the resistance of each cell. Further, an unpopular diagnostic method, galvanostatic charging method, is used to analyze the consistency in further detail. Based on these methods, all four indexes can be directly calculated, and the voltage drop can be accurately separated into three parts.

$$\Delta U_{cell\ i,\ ohmic} = i \times \Delta R_{cell\ i} \tag{2}$$

Fig. 3 shows a typical fuel cell equivalent circuit model. When a high-frequency voltage is applied to this system, it can be simplified into a single-membrane resistance. Based on Ohm's law, Eq. (2) shows the conductivity decline of each membrane. Fig. 4 presents the EIS results of a multi-cell stack. The high-frequency impedance can easily be used to calculate the resistance of the proton exchange membrane. Sometimes, EIS is also used to estimate other parameters [58]. However, it is not recommended in this step for quantitative analysis because EIS is very sensitive to the operating conditions. Even a small change in the inter status can significantly affect the low-frequency test results, and the equivalent circuit model for the low-frequency response remains a matter of debate. Moreover, when using EIS to analyze performance, EIS can be regarded as an extension of the polarization curve. Thus, only the high-frequency resistance is clear and well accepted.

ECSA and crossover tests are difficult for large-scale multi-cell stacks. Traditional CV and LSV methods are the most convenient way to estimate the ECSA and crossover. However, these methods cannot control the voltage change rate of each cell in a multi-cell stack. In

order to obtain an ECSA value for every cell in situ, a novel GSC method was developed to analyze consistency. The test conditions of GSC are similar to those of CV and LSV. Ref. [30] proposed a detailed test process to ensure credible results. Unlike CV, which uses voltage as the controlled variable to analyze the variation trend of the current, the current is the controlled variable in GSC.

Eq. (3) presents the mechanism of GSC, in which the charging current can be consumed by three parts, the desorption of hydrogen on the surface of platinum catalyst (dQ_H), the charge of the double layer capacitance ($C_{dl}dV$), and the hydrogen crossover current (i_{H2}).

$$I_{GA} = \frac{dQ_H + C_{dl}dV + i_{H_2}dt}{dt} = (dQ_H + C_{dl})\frac{dV}{dt} + i_{H_2} \tag{3}$$

$$\begin{cases} I_{GA}|_1 = C_{dl}\frac{dV}{dt}\Big|_1 + i_{H_2} \\ I_{GA}|_2 = C_{dl}\frac{dV}{dt}\Big|_2 + i_{H_2} \\ \quad \cdots\cdots \\ I_{GA}|_n = C_{dl}\frac{dV}{dt}\Big|_n + i_{H_2} \end{cases} \tag{4}$$

$$Q_H = \int_0^{\bar{V}} \left(\frac{I_{GA} - i_{H_2}}{dV/dt} - C_{dl} \right)dV \tag{5}$$

Fig. 5a) shows the voltage curve and derivative voltage curves, dV/dt. The rate of increase in the voltage means the electrochemical reaction rate. Fig. 5b) shows the dV/dt curves under different charging currents. The peak indicates the end of hydrogen desorption process. At this point, dQ_H can be ignored, and only two variables, C_{dl} and i_{H2}, are unknown. Therefore, a least-squares algorithm is applied to fit all the charging peak points in Eq. (4) and Fig. 5c). After obtaining C_{dl} and i_{H2}, ECSA can be easily calculated using Eq. (5).

GSC thus seems to be very convenient for multi-cell analysis. However, this method is still not very popular. Its main bottleneck is that this method requires some special equipment and an intelligent data processing method. Ref. [30] analyzed the effect of test conditions.
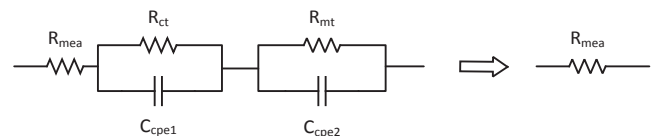

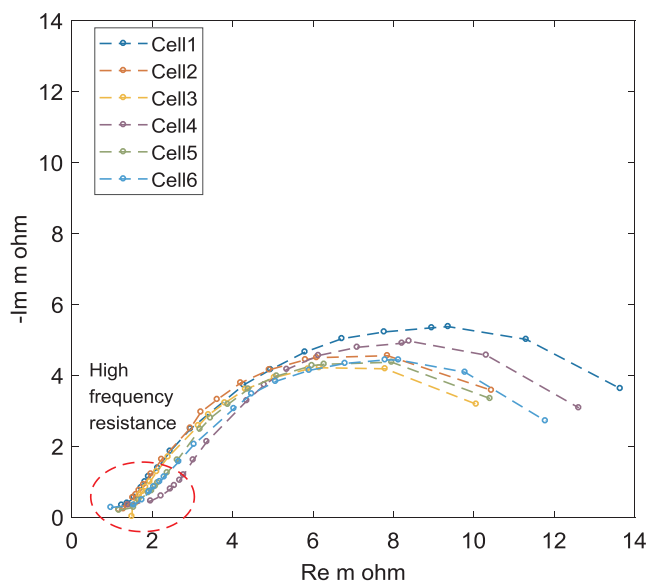**Fig. 3.** Fuel cell equivalent circuit model.

**Fig. 4.** EIS analysis for a multi-cell stack.

High humidity, high temperature, the actual gas pressure during operation, and a high-precision galvanostatic source are necessary for accurate results. Additionally, a data processing method was proposed to decrease the measurement error; however, the most significant challenge for GSC is still the data accuracy, although a galvanostatic power source that was previously shown to be accurate is used in this test. The signal noise cannot be ignored and requires a filter. Therefore, designing a high-efficiency filter is important to the GSC method. Fig. 5d) shows the dV/dt curves before and after a low-pass filter, which demonstrates that most of the noise can be removed from the signal. However, this filter requires considerable computation. For example, the calculation time for a ten-cell stack test is about 10 h. Nevertheless, it can effectively provide a credible result.

With these methods, resistance, ECSA, crossover current and double-layer capacitance of each cell can be obtained. According to the voltage model, the activation loss of every cell can be separated from the voltage drop, as shown in Eq. (6). In addition, the crossover current can be used to analyze the OCV drop and membrane corrosion and to predict the lifetime.
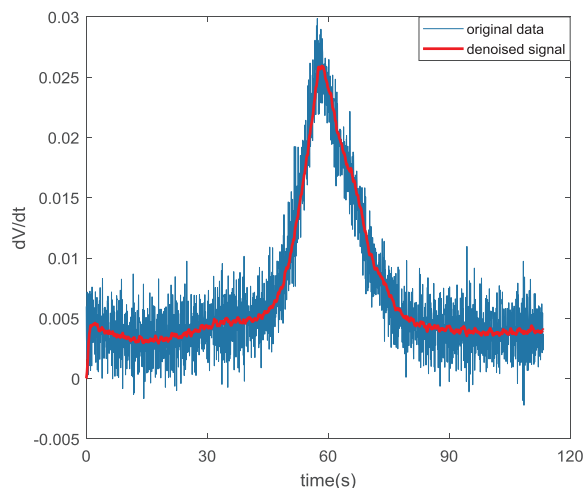
$$\Delta U_{act} = \frac{RT_{fc}}{\alpha_c F} \ln\left(\frac{S_{ECSA1}}{S_{ECSA2}}\right) \tag{6}$$
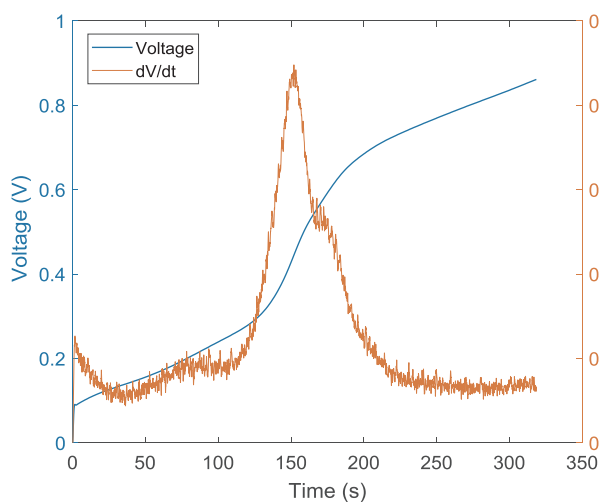
a) Charging curve and dV/dt curve
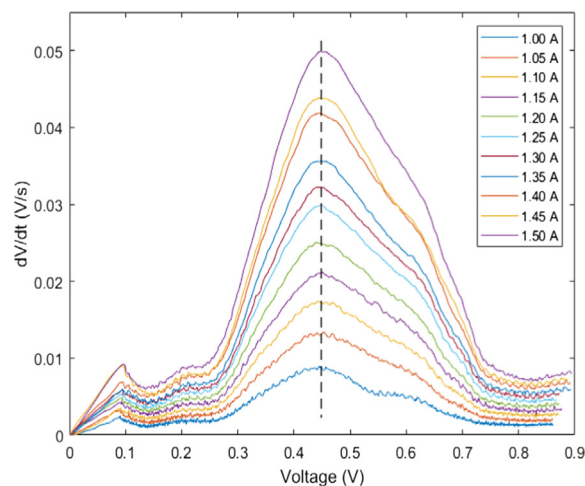
b) Comparison of different charging currents
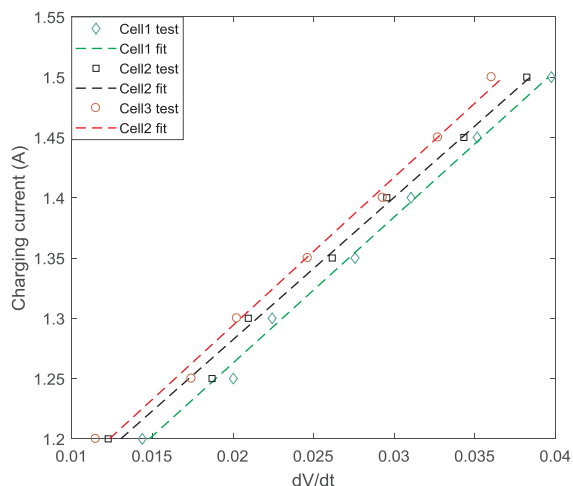
c) ECSA and crossover current estimation

d) Noise processing

Fig. 5. GSC analysis method.

$$\Delta U_{cell\ i,\ concentration} = \Delta U - \Delta U_{cell\ i,\ activation} - \Delta U_{cell\ i,\ ohmic} \quad (7)$$

In Eq. (7), the rest of the voltage drop is considered to be the increasing concentration loss. Based on the two methods, all three overpotentials of each cell can be measured quantitatively, and the cell consistency can be a comprehensively analyzed from these results. In order to clarify this method, this paper presents a case to validate it.

Fig. 6a) shows two average polarization curves of a ten-cell stack. Between the two tests, this fuel cell stack experienced a calendar life test. An obvious voltage drop can be observed in this figure. Based on the qualitative analysis, a brief result can be concluded, that is, the concentration overpotential increases considerably in this fuel cell stack. However, determining what leads to performance degradation is difficult using the calendar life test. In contrast, using the two methods above, the resistance, ECSA, and crossover current were obtained.

Table 1 shows the results of resistance under different output currents. Clearly, the resistance does not increase after the AST test; indeed, even a slight decrease can be observed. Because the resistance is related to the initial status, such resistance fluctuation is acceptable. In addition, the resistance measurement shows that the voltage drop is not caused by an increase in the ohmic loss or membrane degradation.

Table 2 shows the GSC results. An obvious ECSA drop, over a 10% loss, was observed after the calendar life test. According to Eq. (1), the voltage drops by about 5–10 mV due to a loss in the ECSA. However, the real voltage drop is still much larger than the increase in the activation overpotential. Fig. 6b) shows the three parts under two different currents, 500 mA and 1300 mA. The concentration loss is about 10 times higher than the activation loss, which means that the microstructure of the CCL or GDL was destroyed by the calendar life test, which increases the length of the oxygen transport path.

This result provides a comprehensive explanation of the calendar life test. Although the conductivity of the membrane is still normal, the microstructure of GDL or CCL may be damaged, which caused the ECSA to drop rapidly, thereby rapidly increasing the concentration loss.

2.3. Step three: uniformity analysis

In the first two steps, each index does not consider the cell uniformity. However, the degradation rate is not homogeneous in a large-format fuel cell stack, and the non-uniform internal status in high-power fuel cell stacks is the unique factor accelerating the degradation rate. Therefore, the cell uniformity change should also be considered when analyzing performance degradation. Some special cell uniformity

Table 1
High-frequency resistance of a fuel cell.

Current density (A/cm^2)	0	0.1	0.3	0.5	0.8	1	1.3
Test 1 (mΩ·cm^2)	105.0	112.3	99.1	87.9	87.3	88.4	88.9
Test 2 (mΩ·cm^2)	89.5	93.0	85.6	83.3	85.1	86.8	87.2

analyses can provide a useful clue for analyzing the cell failure mode.

However, cell uniformity analyses methods are scarce for commercial fuel cell stacks. All traditional test methods require a specially designed bipolar plate, which may change the original substance distribution, to obtain the internal status distribution. To diagnose commercial fuel cell stacks, any such structural change is forbidden. In this paper, a multi-point voltage monitoring method is applied to analyze the uniformity of a commercial multi-cell stack. This method does not require changing the structure of the bipolar plate but simply adds another set of voltage monitors. With this method, the current and voltage distribution of the failed cell can be obtained.

Fig. 7a) shows a schematic diagram of the multi-point monitoring method. Two sets of voltage monitors were placed along the channel direction in the fuel cell stack. Therefore, each cell has two voltage values, and the voltage distribution is used to index the fuel cell stack consistency and uniformity change. Three principles underlie the multi-point voltage monitoring method mechanism.

- Most bipolar plates are not equipotential bodies;
- Only the two end bipolar plates are equipotential; and
- The total current of each cell is the same.

In previous research, graphite bipolar plates were treated as equipotential bodies. Meanwhile, for analyzing the degradation of large-format multi-cell stacks, the current distribution is different for every cell because the internal status distribution of each cell is also different. Especially for the abnormal cell, there may be an extreme current concentration. If the ideal current distributions in the neighboring cells are different, Fig. 7b) shows that there will be a horizontal direction current in the bipolar plate to balance this requirement. The current flow in the bipolar plate is based on the potential gradient, which also obeys ohmic rules. The resistance in the horizontal direction is much larger than that in the vertical direction. In this way, bipolar plates cannot be treated as equipotential bodies, and the voltage difference in the bipolar plate may cause an error in the cell consistency analysis.
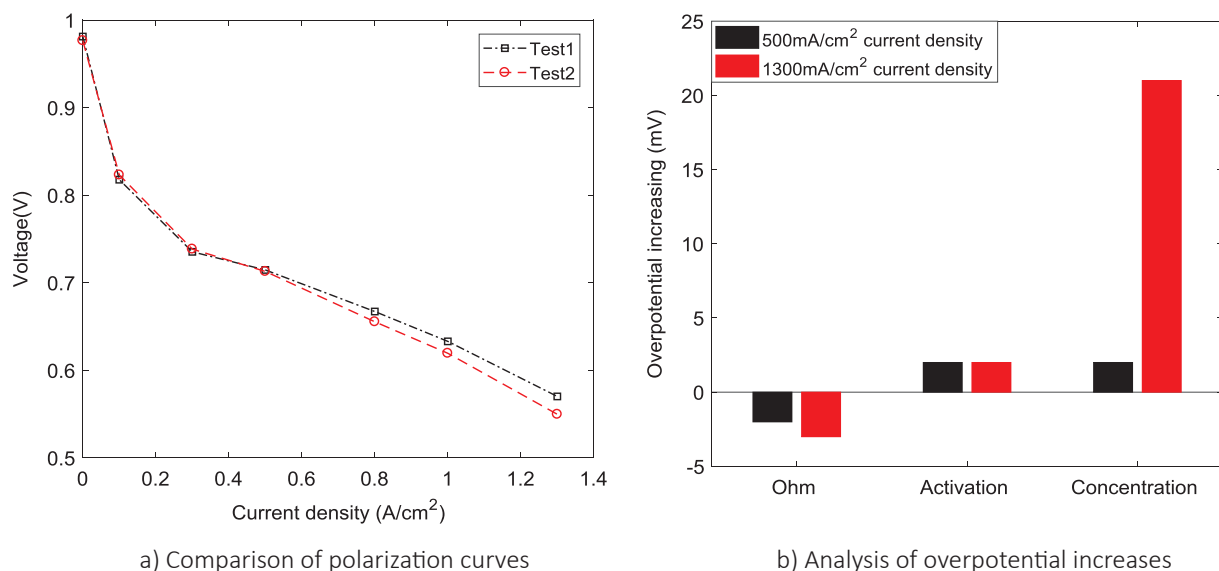

a) Comparison of polarization curves

b) Analysis of overpotential increases

Fig. 6. GSC and EIS analysis demonstration.

Table 2
GSC results.

	Cell 1	Cell 2	Cell 3	Cell 4	Cell 5	Cell 6	Cell 7	Cell 8	Cell 9
ECSA for test 1	36.83	35.25	34.22	35.41	32.73	36.94	36.09	36.76	39.22
ECSA for test 2	31.28	30.50	29.32	28.73	28.78	31.28	30.27	30.76	33.06
Crossover for test 1	0.82	0.83	0.82	0.85	0.83	0.83	0.83	0.83	0.87
Crossover for test 2	0.87	0.88	0.89	0.92	0.89	0.89	0.90	0.89	0.91
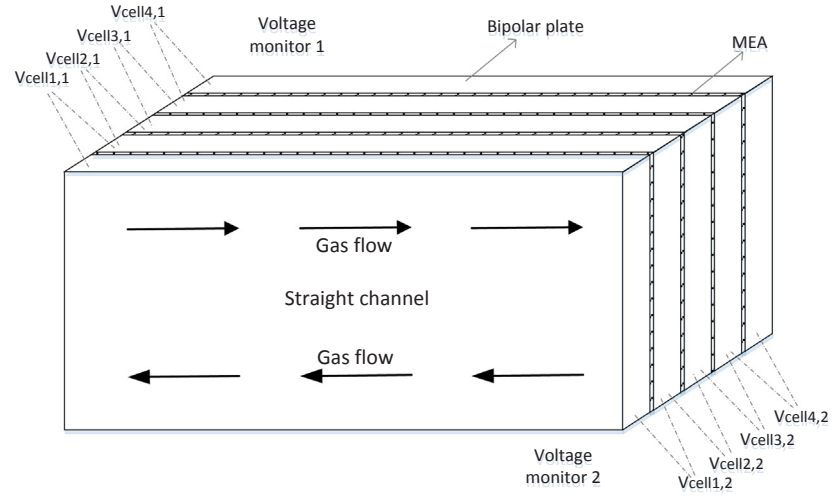
a) Structural framework
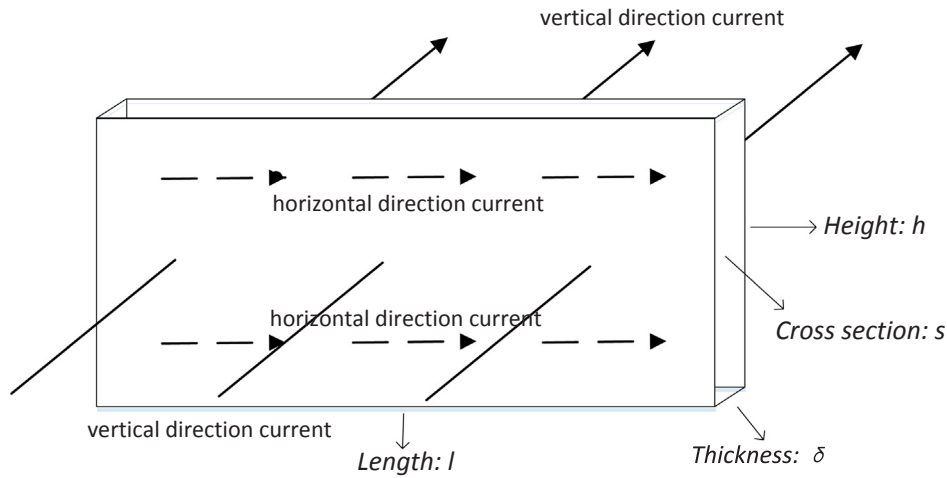
b) Bipolar plate current flow

Fig. 7. Multi-point voltage monitoring method frame.

$$U_i(x) = \sum_{j=1}^{i} V_{cell(j)}(x) \tag{8}$$

$$R_{cross} = \frac{1}{\sigma} \times \frac{l}{s} \tag{9}$$

$$\Delta U_{cell,i} = I_{cross} \times R_{cross} = \left(\Delta i_{cell} \times \frac{1}{2} \times l \times h \right) \times R_{cross} = \Delta i_{cell} \times \frac{l^2}{2\sigma\delta} \tag{10}$$

Eq. (8) shows the potential calculation of each bipolar plate, where V_{cell} is measured with the multi-point voltage monitors. Note that the two bipolar plates at the ends are different from the other plates because the end plate is connected to the copper current collector, which

has very high conductivity. Any potential difference in the end bipolar plate can lead to a very large horizontal current. Therefore, only these two end bipolar plates can be treated as equipotential bodies. Cell 1 connects to the negative electrode, and $V_{cell1}(1)$ and $V_{cell1}(2)$ can be regarded as 0 V. Eq. (9) shows how to calculate the resistance for the horizontal current, where s is the cross-section, and l is the length of the bipolar plate. Compared with that for the vertical current, the cross-section for the horizontal current is smaller, and the length is longer, which is why a small horizontal current can lead to an obvious voltage difference in the bipolar plate.

Eq. (10) presents a function relating the current density difference and the bipolar plate structure. For a fixed current density difference between neighboring cells, the voltage difference between the two

monitors depends on the conductivity, thickness, and length of the bipolar plate. The width of the bipolar plate does not affect the voltage difference. In order to obtain a high-power density, bipolar plates are made to be thinner and larger. The length of the bipolar plate is the main factor for the multi-point voltage monitoring method. For high-power commercial fuel cell stacks, the bipolar plate can be four or five times longer. Considering that the inhomogeneity of the internal status in a longer channel is also larger, the voltage difference in the bipolar plate can be even larger, and this new method should be very effective for large-format multi-cell stacks.

Fig. 8 shows the ΔU–ΔI curves for different bipolar plate structures, which can help to provide a direct understanding of this new method. The black line is the baseline with a graphite bipolar plate, 13 μΩ·m conductivity, 0.2 m in length and 2 mm in thickness. Considering the output current of a fuel cell can reach 1.5 A/cm^2, a difference in the current density difference of 1% in the baseline bipolar plate can reach 20 mV, and a 10% deviation can even lead to a voltage difference of over 100 mV between the two monitors. Especially for the 40 cm bipolar plate, a 1% current density deviation requires a 100 mV potential difference to balance it. These results confirm that the multi-point monitoring method is necessary for analyzing large-format multi-cell stacks. However, if the bipolar plate is only 10 cm long, which is normal for a square bipolar plate, this signal is too weak and cannot be used for the diagnosis. According to engineering experience, coated stainless steel is even less conductive than graphite. Therefore, this method also can be used for fuel cell stacks with metal bipolar plates.

Cell consistency and uniformity are coupled in a multi-cell stack. The exacerbation of the cell non-uniformity is the root of cell inconsistency, which can lead to a redistribution of current and voltage in the bipolar plate. Given that the potential in the bipolar plate is variable, one set of voltage monitors can explain the potential distribution of bipolar plate, which sometimes may mislead researchers [57]. On the other hand, the voltage redistribution resulting from cell interaction can also work as an efficient index for the fuel cell SOH, which can help to analyze the current distribution in fuel cell stacks.

Fig. 9 shows the analysis process of the multi-point voltage monitoring method. According to the voltage values from the two sets of monitors, the horizontal current in each bipolar plate can be easily obtained. The next step is to judge whether current is concentrated in a certain region in this fuel cell stack. Previous research shows that if one cell is abnormal, the voltage difference in this abnormal cell is much larger than that of the other cells. The current flow in the bipolar plates can confirm the current concentration of the abnormal cell. Finally, a more detailed explanation of the current concentration should be concluded from multi-point voltage monitoring method analysis [59]. Performance degradation resulting from membrane dehydration, flooding, fuel starvation, air starvation, and temperature non-uniformity can show different current distribution characteristics. Combined with the operating conditions and the current concentration results, this method can comprehensively analyze the failure mode of the abnormal cell.

Note that the multi-point voltage monitoring method is not used to directly obtain the internal current distribution of all cells but rather the uniformity difference resulting from cell consistency. For an abnormal cell, this method can point out the region of high-current concentration in this stack. These characteristics are important to the fuel cell stack analysis because the voltage redistribution processes are sometimes deceptive and dangerous for multi-cell stacks.

Previous research shows that a multi-point monitoring method can be useful for diagnosing some extreme conditions, such as fuel starvation [57]. Fig. 10 shows that when one cell suffers fuel starvation, most of the current will be concentrated in the anode inlet region. Such an extreme current distribution can significantly affect the potential distribution in the bipolar plate. If the voltage monitor is placed in the anode inlet region, the voltage difference between a normal cell and the fuel-starved cell is less than 200 mV, while in the anode outlet region, it

can be more than 600 mV. These two different conditions are both dangerous. Only one set of voltage monitors may easily mislead the diagnostic system, and thus, the multi-point monitoring method is very convenient and accurate for diagnosing all extreme conditions.

2.4. Degradation analysis framework

According to the analysis above, a comprehensive degradation analysis system for multi-cell fuel cell stacks is proposed in Fig. 11. This diagnostic methodology consists of three steps. All these technologies are easy to conduct and do not require a structural redesign. On the other hand, this diagnostic methodology combines quantitative and qualitative methods. Specifically, step one is a rapid qualitative judgment, step two is a quantitative cell consistency analysis, and step three is a qualitative cell uniformity analysis.

In addition, step one is the basis for the next two steps. A polarization curve can rapidly provide guidance for the diagnostic analysis. Furthermore, the polarization curve test is convenient and inexpensive and thus suitable for high-power fuel cell stacks. However, step one cannot directly quantify fuel cell health. In step two, some quantitative methods are adopted to obtain the internal parameters of each cell. During this step, GSC and EIS provide convenient approaches to monitor the MEA health. According to changes in the core parameters, a brief analysis of the component degradation can be obtained for all cells. In the last step, a special multi-point monitoring method is used to clarify the change in the uniformity of the failed cell. Cell consistency and uniformity are coupled in multi-cell stacks. This step can obtain the real internal current and voltage distribution in a fuel cell stack, and it provides a detailed analysis of the failed cell.

In conclusion, this diagnostic methodology can comprehensively analyze the internal heterogeneity of a fuel cell stack, which is the main difference between single small cells and large-format fuel cell stacks. An effective methodology to diagnose fuel cell stack consistency and uniformity degradation is key to optimizing the service life of fuel cell stacks.

3. Conclusion

In summary, this paper proposed an in situ methodology to diagnose the health of a fuel cell stack. This methodology can provide a quantitative–qualitative internal heterogeneity analysis for large-format commercial fuel cell stacks.
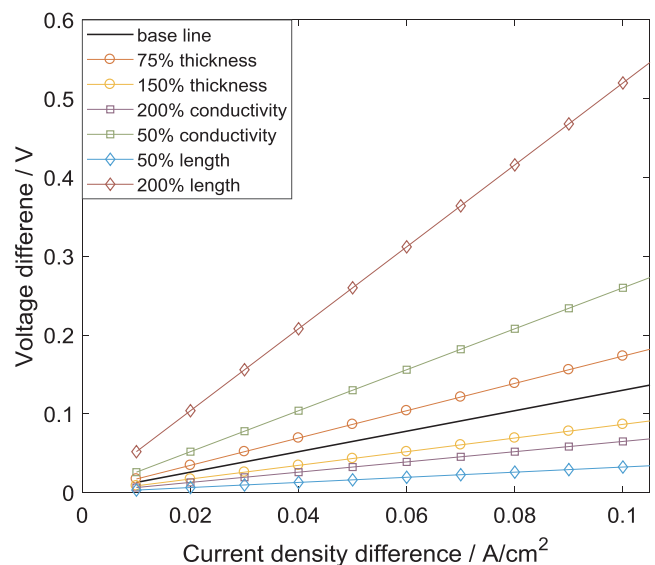

Fig. 8. Voltage difference as a function of cross-plate current density difference for various bipolar plate structures.

$$U_{BPi,1} = \sum_{j=1}^{i} V_{cell\,i,1} \quad U_{BPi,2} = \sum_{j=1}^{i} V_{cell\,i,2}$$

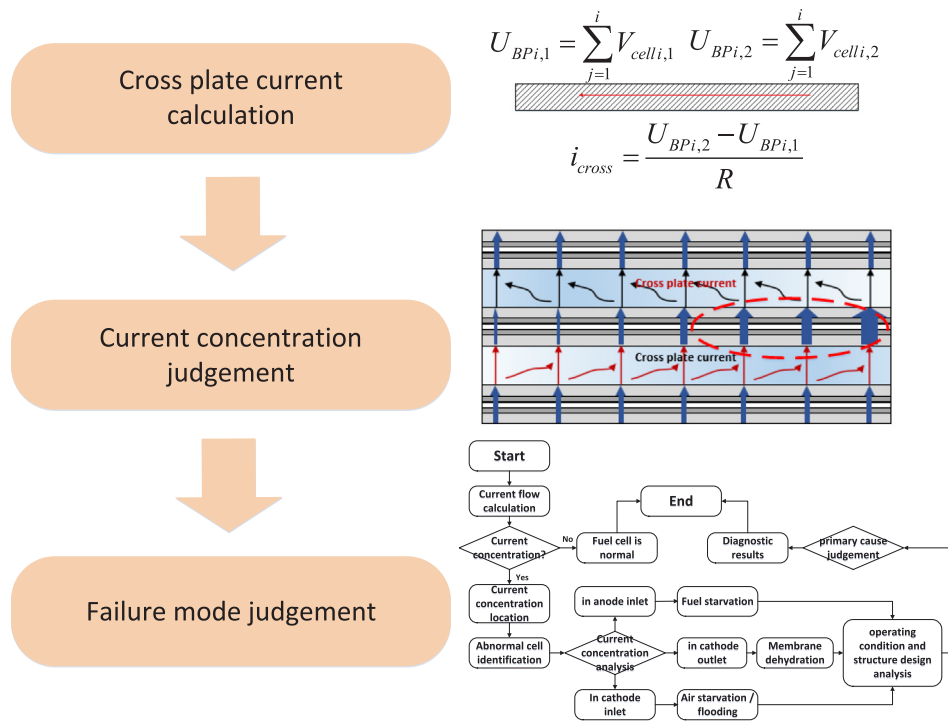$$i_{cross} = \frac{U_{BPi,2} - U_{BPi,1}}{R}$$

Fig. 9. Multi-point voltage monitor method analysis framework.

This novel analytical methodology consists of three steps. Step one uses a polarization curve analysis to provide qualitative guidance for the next two steps. Step two focuses on analyzing cell consistency. Some special diagnostic methods, namely, GSC and EIS, are used to obtain the consistency in the internal parameters of each cell. Step three attempts to explain the cell uniformity degradation. This step introduces a new method, the multi-point monitoring method, to identify the current and voltage distribution of the abnormal cell. None of the technologies in this system require changing the structural design of fuel cell stacks and can be applied directly to large-format multi-cell stacks.

Engineering experience shows that the reasons for degradation in multi-cell stacks are very complex. In addition, some special cases may not be explained by this diagnostic system. In the future, more useful technologies should be added to this methodology to enrich this analysis system. Particularly for the uniformity analysis, this new method can only be used to diagnose abnormal cells. Obtaining the current
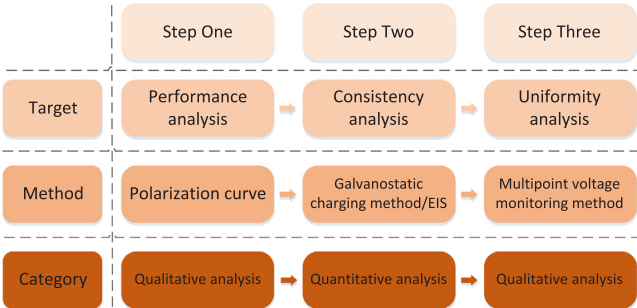

Fig. 11. Multi-cell stack internal heterogeneity analysis frame diagram.
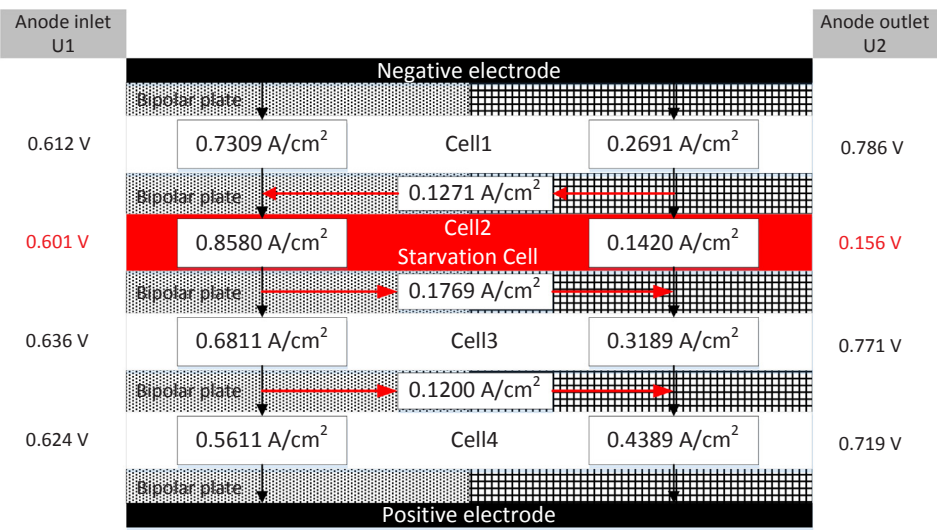

Fig. 10. Current distribution under fuel starvation.

distribution of all cells in situ, however, remains a challenge.

Declaration of interests

Acknowledgement

References

[1] Wang Y, Chen KS, Mishler J, Cho SC, Adroher XC. A review of polymer electrolyte membrane fuel cells: technology, applications, and needs on fundamental research. Appl Energy 2011;88(4):981–1007.

[2] Lü X, Qu Y, Wang Y, Qin C, Liu G. A comprehensive review on hybrid power system for PEMFC-HEV: issues and strategies. Energy Convers Manage 2018;171:1273–91.

[3] Bizon N, Thounthong P. Fuel economy using the global optimization of the Fuel Cell Hybrid Power Systems. Energy Convers Manage 2018;173:665–78.

[4] Sequeira CAC, Brito PSD, Mota AF, Carvalho JL, Rodrigues LFFTTG, Santos DMF, et al. Fermentation, gasification and pyrolysis of carbonaceous residues towards usage in fuel cells. Energy Convers Manage 2007;48(7):2203–20.

[5] Hu Z, Xu L, Li J, Ouyang M, Song Z, Huang H. A reconstructed fuel cell life-prediction model for a fuel cell hybrid city bus. Energy Convers Manage 2018;156:723–32.

[6] Hu Z, Li J, Xu L, Song Z, Fang C, Ouyang M, et al. Multi-objective energy management optimization and parameter sizing for proton exchange membrane hybrid fuel cell vehicles. Energy Convers Manage 2016;129:108–21.

[7] Zhang HF, Pei PC, Yuan X, Chao PX, Wang XZ. Regularization of the degradation behavior and working zone of proton exchange membrane fuel cells with a five-constant ideal cell as prototype. Energy Convers Manage 2011;52(10):3189–96.

[8] Wu J, Yuan XZ, Martin JJ, Wang H, Zhang J, Shen J, et al. A review of PEM fuel cell durability: degradation mechanisms and mitigation strategies. J Power Sources 2008;184(1):104–19.

[9] Xu L, Reimer U, Li J, Huang H, Hu Z, Jiang H, et al. Design of durability test protocol for vehicular fuel cell systems operated in power-follow mode based on statistical results of on-road data. J Power Sources 2018;377:59–69.

[10] Yuan XZ, Zhang S, Wang H, Wu J, Sun JC, Hiesgen R, et al. Degradation of a polymer exchange membrane fuel cell stack with Nafion® membranes of different thicknesses: Part I. In situ diagnosis. J Power Sources 2010;195(22):7594–9.

[11] Hu Z, Xu L, Song Z, Li J, Ouyang M. A semiempirical dynamic model of reversible open circuit voltage drop in a PEM fuel cell. Int J Energy Res 2018.

[12] Yu S, Li X, Li J, Liu S, Lu W, Shao Z, et al. Study on hydrophobicity degradation of gas diffusion layer in proton exchange membrane fuel cells. Energy Convers Manage 2013;76:301–6.

[13] Borup RL, Vanderborgh NE. Design and testing criteria for bipolar plate materials for PEM fuel cell applications. MRS Online Proceedings Library Archive 1995;393.

[14] Pei P, Chen H. Main factors affecting the lifetime of Proton Exchange Membrane fuel cells in vehicle applications: a review. Appl Energy 2014;125:60–75.

[15] Dubau L, Castanheira L, Maillard F, Chatenet M, Lottin O, Maranzana G, et al. A review of PEM fuel cell durability: materials degradation, local heterogeneities of aging and possible mitigation strategies. Wiley Interdiscip Rev: Energy Environ 2014;3(6):540–60.

[16] Marx N, Boulon L, Gustin F, Hissel D, Agbossou K. A review of multi-stack and modular fuel cell systems: interests, application areas and on-going research activities. Int J Hydrogen Energy 2014;39(23):12101–11.

[17] Wang B, Wu K, Yang Z, Jiao K. A quasi-2D transient model of proton exchange membrane fuel cell with anode recirculation. Energy Convers Manage 2018;171:1463–75.

[18] Li J, Hu Z, Xu L, Ouyang M, Fang C, Hu J, et al. Fuel cell system degradation analysis of a Chinese plug-in hybrid fuel cell city bus. Int J Hydrogen Energy 2016;41(34):15295–310.

[19] Jang JH, Chiu HC, Yan WM, Sun WL. Effects of operating conditions on the performances of individual cell and stack of pem fuel cell. J Power Sources 2008;180(1):476–83.

[20] Park YH, Caton JA. Development of a PEM stack and performance analysis including the effects of water content in the membrane and cooling method. J Power Sources 2008;179(2):584–91.

[21] Li Y, Zhao X, Liu Z, Li Y, Chen W, Li Q. Experimental study on the voltage uniformity for dynamic loading of a PEM fuel cell stack. Int J Hydrogen Energy 2015;40(23):7361–9.

[22] Jiang H, Xu L, Fang C, Zhao X, Hu Z, Li J, et al. Experimental study on dual recirculation of polymer electrolyte membrane fuel cell. Int J Hydrogen Energy

[23] Candusso D, De Bernardinis A, Péra MC, Harel F, François X, Hissel D, et al. Fuel cell operation under degraded working modes and study of diode by-pass circuit dedicated to multi-stack association. Energy Convers Manage 2008;49(4):880–95.

[24] Yang XG, Ye Q, Cheng P. Matching of water and temperature fields in proton exchange membrane fuel cells with non-uniform distributions. Int J Hydrogen Energy 2011;36(19):12524–37.

[25] Heidary H, Kermani MJ, Dabir B. Influences of bipolar plate channel blockages on PEM fuel cell performances. Energy Convers Manage 2016;124:51–60.

[26] Hou Z, Wang R, Wang K, Shi W, Xing D, Jiang H. Failure mode investigation of fuel cell for vehicle application. Front Energy 2017;11(3):318–25.

[27] Xing L, Du S, Chen R, Mamlouk M, Scott K. Anode partial flooding modelling of proton exchange membrane fuel cells: model development and validation. Energy 2016;96:80–95.

[28] Xing L, Cai Q, Xu C, Liu C, Scott K, Yan Y. Numerical study of the effect of relative humidity and stoichiometric flow ratio on PEM (proton exchange membrane) fuel cell performance with various channel lengths: an anode partial flooding modelling. Energy 2016;106:631–45.

[29] Yang XG, Ye Q, Cheng P. In-plane transport effects on hydrogen depletion and carbon corrosion induced by anode flooding in proton exchange membrane fuel cells. Int J Heat Mass Transf 2012;55(17–18):4754–65.

[30] Hu Z, Xu L, Huang Y, Li J, Ouyang M, Du X, et al. Comprehensive analysis of galvanostatic charge method for fuel cell degradation diagnosis. Appl Energy 2018;212:1321–32.

[31] Wu J, Yuan XZ, Martin JJ, Wang H, Yang D, Qiao J, et al. Proton exchange membrane fuel cell degradation under close to open-circuit conditions: Part I: In situ diagnosis. J Power Sources 2010;195(4):1171–6.

[32] Springer TE, Zawodzinski TA, Gottesfeld S. Polymer electrolyte fuel cell model. J Electrochem Soc 1991;138(8):2334–42.

[33] Nørskov JK, Rossmeisl J, Logadottir A, Lindqvist LRKJ, Kitchin JR, Bligaard T, et al. Origin of the overpotential for oxygen reduction at a fuel-cell cathode. J Phys Chem B 2004;108(46):17886–92.

[34] Barbir F, Gorgun H, Wang X. Relationship between pressure drop and cell resistance as a diagnostic tool for PEM fuel cells. J Power Sources 2005;141(1):96–101.

[35] Qin Y, Du Q, Fan M, Chang Y, Yin Y. Study on the operating pressure effect on the performance of a proton exchange membrane fuel cell power system. Energy Convers Manage 2017;142:357–65.

[36] Mench MM, Kumbur EC, Veziroglu TN, editors. Polymer electrolyte fuel cell degradation. Academic Press; 2011.

[37] Zenyuk IV, Das PK, Weber AZ. Understanding impacts of catalyst-layer thickness on fuel-cell performance via mathematical modeling. J Electrochem Soc 2016;163(7):F691–703.

[38] Pant LM, Yang Z, Perry ML, Weber AZ. Development of a simple and rapid diagnostic method for polymer-electrolyte fuel cells. J Electrochem Soc 2018;165(6):F3007–14.

[39] Xu L, Fang C, Li J, Ouyang M, Lehnert W. Nonlinear dynamic mechanism modeling of a polymer electrolyte membrane fuel cell with dead-ended anode considering mass transport and actuator properties. Appl Energy 2018;230:106–21.

[40] Xu L, Hong P, Fang C, Li J, Ouyang M, Lehnert W. Interactions between a polymer electrolyte membrane fuel cell and boost converter utilizing a multiscale model. J Power Sources 2018;395:237–50.

[41] Yuan X, Sun JC, Blanco M, Wang H, Zhang J, Wilkinson DP. AC impedance diagnosis of a 500 W PEM fuel cell stack: Part I: Stack impedance. J Power Sources 2006;161(2):920–8.

[42] Yuan X, Sun JC, Wang H, Zhang J. AC impedance diagnosis of a 500 W PEM fuel cell stack: Part II: Individual cell impedance. J Power Sources 2006;161(2):929–37.

[43] Darowicki K, Gawel L. Impedance measurement and selection of electrochemical equivalent circuit of a working PEM fuel cell cathode. Electrocatalysis 2017;8(3):235–44.

[44] Martin S, Garcia-Ybarra PL, Castillo JL. Long-term operation of a proton exchange membrane fuel cell without external humidification. Appl Energy 2017;205:1012–20.

[45] Choi W, Enjeti PN, Howze JW. Development of an equivalent circuit model of a fuel cell to evaluate the effects of inverter ripple current. Applied power electronics conference and exposition, 2004. APEC'04. Nineteenth Annual IEEE, vol. 1. IEEE; 2004. p. 355–61.

[46] Lee KS, Lee BS, Yoo SJ, Kim SK, Hwang SJ, Kim HJ, et al. Development of a galvanostatic analysis technique as an in-situ diagnostic tool for PEMFC single cells and stacks. Int J Hydrogen Energy 2012;37(7):5891–900.

[47] Pei P, Xu H, Zeng X, Zha H, Song M. Use of galvanostatic charge method as a membrane electrode assembly diagnostic tool in a fuel cell stack. J Power Sources 2014;245:175–82.

[48] Brightman E, Hinds G, O'Malley R. In situ measurement of active catalyst surface area in fuel cell stacks. J Power Sources 2013;242:244–54.

[49] Torija S, Prieto-Sanchez L, Ashton SJ. In-situ electrochemically active surface area evaluation of an open-cathode polymer electrolyte membrane fuel cell stack. J Power Sources 2016;327:543–7.

[50] Freunberger SA, Schneider IA, Sui PC, Wokaun A, Djilali N, Büchi FN. Cell interaction phenomena in polymer electrolyte fuel cell stacks. J Electrochem Soc 2008;155(7):B704–14.

[51] Abbou S, Dillet J, Maranzana G, Didierjean S, Lottin O. Local potential evolutions during proton exchange membrane fuel cell operation with dead-ended anode-Part I: Impact of water diffusion and nitrogen crossover. J Power Sources 2017;340:337–46.

[52] Abbou S, Dillet J, Maranzana G, Didierjean S, Lottin O. Local potential evolutions during proton exchange membrane fuel cell operation with dead-ended anode-Part

II: Aging mitigation strategies based on water management and nitrogen crossover. J Power Sources 2017;340:419–27.

[53] Yang XG, Burke N, Wang CY, Tajiri K, Shinoharab K. Simultaneous measurements of species and current distributions in a pefc under low-humidity operation. J Electrochem Soc 2005;152(4):A759–66.

[54] Kramer D, Zhang J, Shimoi R, Lehmann E, Wokaun A, Shinohara K, et al. In situ diagnostic of two-phase flow phenomena in polymer electrolyte fuel cells by neutron imaging: Part A. Experimental, data treatment, and quantification. Electrochim Acta 2005;50(13):2603–14.

[55] Litster S, Sinton D, Djilali N. Ex situ visualization of liquid water transport in PEM fuel cell gas diffusion layers. J Power Sources 2006;154(1):95–105.

[56] Hu Z, Xu L, Li J, Gan Q, Xu X, Ouyang M, et al. A multipoint voltage-monitoring method for fuel cell inconsistency analysis. Energy Convers Manage 2018;177:572–81.

[57] Hu Z, Xu L, Li J, Hu J, Xu X, Du X, et al. A cell interaction phenomenon in a multi-cell stack under one cell suffering fuel starvation. Energy Convers Manage 2018;174:465–74.

[58] Kulikovsky AA. Exact low-current analytical solution for impedance of the cathode catalyst layer in a PEM fuel cell. Electrochim Acta 2014;147:773–7.

[59] Hu Z, Xu L, Li J, et al. An in situ diagnostic method for multi-cell fuel cell stack uniformity and consistency analysis, APEN-D-18-11240. 2018. [Under review].